Nuclear Instruments and Methods in Physics Research B 563 (2025) 165696

Contents lists available at ScienceDirect

Nuclear Inst. and Methods in Physics Research, B

journal homepage: www.elsevier.com/locate/nimb

Full Length Article

Performance testing a portable ^{109}Cd XRF system for the measurement of *ex vivo* skin iron content in a rat model of iron overload

Sami Ullah Bangash, PhD [a,*], Fiona E. McNeill [a], Michael J. Farquharson [b], Bruce Wainman [c], Michelle Zeller [d]

[a] Department of Physics and Astronomy, McMaster University, Hamilton, ON L8S 4K1, Canada
[b] School for Interdisciplinary Sciences, McMaster University, Hamilton, ON L8S 4K1, Canada
[c] Department of Pathology and Molecular Medicine, McMaster University, Hamilton, ON L8S 4K1, Canada
[d] Division of Hematology and Thromboembolism, Department of Medicine, McMaster University, Hamilton, ON L8S 4K1, Canada

ARTICLE INFO

Keywords:
XRF
Laboratory XRF
Portable XRF

ABSTRACT

The ability of a ^{109}Cd-based portable X-ray fluorescence (^{109}Cd pXRF) system to differentiate iron (Fe) levels in the ex vivo skin of 28 rats dosed with Fe^{2+} via intraperitoneal injection has been tested. The 28 animals included control rats and those dosed with either 80 mg Fe^{2+}/kg or 160 mg Fe^{2+}/kg. The system was able to distinguish between groups of control and dosed rats based on their measured skin iron concentration ($p = 0.001$ and $p = 0.002$). Further, linear regression analysis of individual rat skin Fe levels against Fe^{2+} dose in mg/kg showed a strong correlation ($r^2 = 0.84$, $p < 0.0001$) and indicated that the system could determine whether individual animals had been dosed with Fe. Strong correlation ($r^2 = 0.85$, $p < 0.0001$) between the ^{109}Cd pXRF system skin Fe measurements and skin Fe measurements using a laboratory-based XRF system (which had previously shown a correlation between skin Fe and with liver Fe) suggest that ^{109}Cd pXRF measurements could be used to predict elevated Fe levels in the liver.

1. Introduction

Fe is an essential element that regulates many physiological functions in the body however, Fe overload leads to critical organ failure. Peak serum Fe levels of less than 350 μg/dl are considered minimally toxic, while levels greater than 500 μg/dl are classed as severe toxicity [1]. Fe overload causes organ damage as a result of deposition of Fe in the tissues. Organs susceptible to damage from Fe deposition include the liver, pancreas, heart, skin and pituitary gland. There are numerous diseases where patients are monitored and treated for Fe overload. β-thalassemia and hereditary hemochromatosis, are examples of genetic disorders that require long-term monitoring of Fe levels because both patient populations can experience Fe overload (although for different reasons). β-thalassemia is an inherited disorder in which the formation of β-globin chains in hemoglobin are reduced. Clinical presentations vary depending on genetic profile and how many β-globin genes are impacted. Patients with thalassemia major are dependant upon repeated blood transfusion due to life-long and severe anemia. Multiple blood transfusions in the absence of bleeding places these patients at risk of Fe overload as each transfused unit of red blood cells (RBCs) contains Fe. Hereditary hemochromatosis is a genetic disorder in which the body absorbs too much Fe from the intestine, accumulating excess Fe in critical organs [2]. Accurate monitoring of Fe levels is essential in both these groups of patients and in some other disorders. As has been described in a prior publication [3], there are currently limitations to the available clinical methods for the assessment of Fe overload [4]. Blood tests, MRI imaging and biopsy of different tissues and organs are currently used to measure Fe levels in the body; each of these methods have limitations including: results being affected by bacterial or viral infection (blood); cost and availability (MRI and SQUID); and risk of infection (biopsy). None of these technologies provide immediate results and so referring the patient for tests, and discussing results with the patient, requires two separate appointments with a physician, increasing costs and incurring delays. New technologies that permit rapid, accurate, reproducible and minimally invasive point-of-care assessment of Fe levels in vivo are urgently needed to provide effective and efficient care to patients with Fe overload.

* Corresponding author.
E-mail address: bangashs@mcmaster.ca (S.U. Bangash).

https://doi.org/10.1016/j.nimb.2025.165696
Received 17 September 2024; Received in revised form 7 March 2025; Accepted 29 March 2025

1.1. In vivo X-ray fluorescence

X-ray Fluorescence (XRF) is a measurement technique that has been widely used to measure elements in vivo [4]. The premise of XRF is simple: a sample or person is irradiated with x- or γ-rays of energy above the absorption edge of the element of interest, and the subsequent characteristic x-rays are measured. In practice, accurate measurement in vivo is complex and challenging because the low average atomic number of human tissues often means that background signals from Compton scattering can be large, leading to poor signal to noise ratios. In addition, people present in a wide variety of shapes and sizes and so quantitation is often performed by comparing the signal from a person with the signal from an anthropomorphic phantom of known concentration that matches the size, shape and elemental composition of the person. However, rather than directly comparing x-ray signals of an in vivo measurement against an anthropomorphic phantom to estimate concentration, some researchers have taken a different analysis approach and employed a fundamental parameter method for XRF, using cross-section data, knowledge of the excitation spectrum and measurements of detector broadening to evaluate concentrations [5–7]. In either approach, measurements must be validated, and effort has been spent over the last few decades on the development of appropriate phantoms [8] and/or reference standards [9].

However, despite the challenges, XRF systems have been successfully developed. For example, measurements of lead in bone have been used for over 40 years to safely assess long-term or chronic lead exposure [10–14], while studies of uranium in bone were used to study the exposure of veterans from the Gulf War in the 1990s [15,16]. These early XRF systems used radioisotope sources, but more recently the use of hand-held XRF systems have been developed and applied to the study of lead and strontium in bone in vivo [17–25]. These hand-held systems have been shown to perform significantly better than radioisotope systems for systems such as the measurement of strontium in bone [26], but the improved detection limit comes at a cost of significantly higher radiation dose. The proven utility of the XRF technique means that many researchers have attempted to develop systems to measure iron in vivo and some systems been successfully applied in the measurement of iron in vivo in animals and humans [27–33,3].

The systems that have been previously tested for the study of iron in vivo include the use of a ^{238}Pu x-ray source with an Si-PIN photodiode detector in a human study of patients with iron overload disease [27]. This system reported a detection limit of 13 ppm and delivered a dose of 10 mSv to the skin. People's skin was measured three times for 50 s and an average estimate calculated. The authors of this human study also report using the device successfully in mice to identify infection but did not report radiation dose data [34]. A recent study reported the use of a commercial hand-held x-ray device (an Olympus Delta Professional XRF Analyzer) to measure iron in the skin of rats in vivo [32]. This system employed a small x-ray tube and measurements were made at incident energies of 40 and 15 keV. The study did not report a detection limit but instead reported measurement uncertainties of 0.3 % in the iron signal from control rats. However, data provided in the publication [32] show that the measurement uncertainty rose significantly in iron-dosed animals, and the average skin dose for a 30 s measurement at an operating voltage of 15 keV was high, 87 ± 20 mSv [32], and so further development of the system was ceased.

This initial in vivo study [32] using the commercial hand-held device did, however, yield valuable data. The researchers performed ex vivo measurements of iron levels in the skin, liver and kidney of rats that had been sacrificed after in vivo measurement. They found that skin Fe concentration correlated to liver Fe concentration [32], corroborating an earlier ex vivo XRF study which found correlations between skin iron and liver iron levels in rats [35]. The relationship between skin iron level and liver iron level has also been demonstrated in other studies using a variety of techniques [35–39].

There is good evidence therefore that an elevated skin iron level correlates to an elevated liver iron level and a technology that can accurately identify whether Fe levels in the skin are elevated could potentially be predictive of risk to a critical organ, the liver. We have developed a portable device for measurement of Fe in the skin using ^{109}Cd based X-ray fluorescence (^{109}Cd pXRF) [3]. The system has shown potential utility and has been demonstrated accurate [33]. In this article we report the results of testing the performance of the ^{109}Cd pXRF system in assaying the Fe skin levels of rats dosed with varying levels of Fe.

The researchers who had used the commercial hand-held x-ray device to study Fe levels in the skin of rats both in vivo and ex vivo [32] had archived ex vivo samples in a −80° freezer. The archived samples were made available for this study. The ^{109}Cd pXRF system was used to measure the Fe levels of these archival ex vivo rat skin samples and was tested to see if it could be intercalibrated with a laboratory-based XRF system. This opportunistic use of existing samples was considered an ethical method of testing the system as it avoided the sacrifice of further animals. However, it should be noted that the Fe dosing of the rats was designed for the prior study and was not necessarily best tailored for the work presented here. However, it was decided that these rat skin sample measurements would allow the predictive capabilities of the system in skin to be tested. As prior ex vivo measurements with the laboratory system had shown correlations between skin and liver Fe levels in individual animals, inter-calibration of skin Fe measurements using the ^{109}Cd pXRF system against skin Fe levels in the laboratory-based system aimed to show that the ^{109}Cd pXRF results could be inferred to be predictive of levels in organs at risk such as the liver. The goal was to determine whether the system was able to distinguish between the skin Fe levels of groups of rats dosed with varying levels of Fe or possibly whether the system was able to distinguish between the Fe levels of individual animals.

1.2. Comparison of rat and human skin

The question of whether the results of testing the system in rats is predictive of performance of the system in measurements in human skin is dependent on the similarities between rat and human skin. The choice of an animal as a model in a pre-clinical study depends on how easily they can be handled, their cost and availability. Since rats are inexpensive, readily available, and have skin similarities to humans, they were used as a model to study Fe overload conditions in the prior XRF study [32].

As shown in Fig. 1, the epidermis, the outer layer of skin, is subdivided into four distinct sublayers: the basal layer (deepest), spinous layer, granular layer, and the stratum corneum (the most superficial layer) [39]. The stratum corneum is a thin layer of dead cells. In both human and rat skin, the cells within this layer have lost their nuclei and organelles. These cells, called keratinocytes, are filled with a protein called keratin, and contain lipids. The primary function of this layer in both types of skin is to prevent excessive water loss and to act as a protective barrier [40]. In rats and humans, keratinocytes in the basal

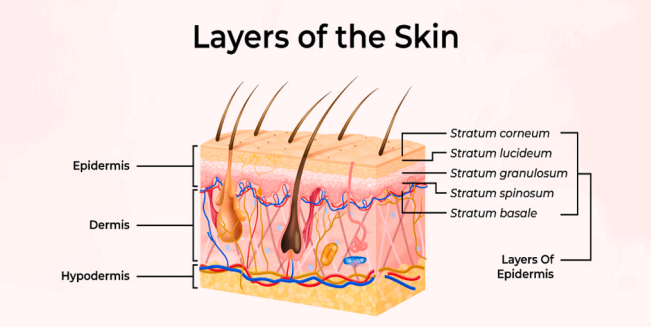

Fig. 1. An illustration of human skin structure depicting the distinct layers of the skin [40].

layer proliferate and migrate toward the surface and both rat and human basal layers contain melanocytes (responsible for pigmentation) and Merkel cells (a type of mechanoreceptor) [40].

Rat skin is generally thinner than human skin, although there is some overlap in the thickness of the epidermis in rats and humans, and in some regions of skin, the thickness of the rat epidermis closely approximates that of human skin. For instance, the thickness of the epidermis on the feet of rats (ranging from 350 to 450 μm) is comparable to the average thickness of the epidermis on the human palm and soles of the feet (ranging from 300 to 400 μm) [41].

The stratum spinosum is present in humans as well as in the thick skin found in rats, such as the skin on their paws [40]. Keratinocytes within this layer continue to differentiate and undergo significant transformation, a process that is similar in both human and rat skin. The next layer, the stratum granulosum, is clearly marked in rat skin. The primary function of this layer in both humans and rats is to act as a protective barrier in skin cells [41].

Beneath the basal layer lies the dermis. The dermis in both rats and humans consists of connective tissues and elastic fibres that provide strength [42]. Both rat and human skin are equipped with nerve endings responsible for sensory perception. The dermis is also supplied with blood vessels to deliver nutrients and oxygen to the skin [40]. However, the density and distribution of blood vessels and nerve endings may be different in rat and human skin. The thickness of the dermis in human skin varies from 1 to 4 mm [42] depending upon the location of the skin, while it ranges from 0.1 mm to 3 mm in rat skin [41]. The boundary between the dermis and epidermis is not flat in human skin; instead, it has downward epidermis extensions, known as rete ridges, that are absent in rat skin [40].

As discussed, humans and rats both have three layers of skin, but rat skin is more loosely attached compared to human skin [43]. This is however a result of the structure of the hypodermis, not the epidermis or dermis. While there is some overlap in epidermal thickness, the average epidermal thickness in rat skin is thinner than in humans as it ranges from approximately 15 to 170 μm with skin being thickest during adolescence [41]. The average epidermal thickness in human skin is approximately 100 μm, with a range of 50 μm–1 mm [44]. However, as previously mentioned, human epidermal thickness varies strongly with location with the thickest skin in the human body being found on the plantar aspect of the foot [8] while the thinnest is found in the pubic and genital areas of the body (average thicknesses 31 and 45 μm) [45]. However, neither of these epidermal thickness extremes are likely sites for a point-of-care in vivo measurement. The more likely sites of the volar or dorsal forearm, wrist or dorsum of the hand, have average thicknesses from 75 to 94 μm. As rat epidermal thicknesses vary from 15 to 170 μm, there is therefore some overlap in the thickness of the human epidermis that would be measured in vivo and the epidermis thickness in rats.

The penetration of 6.4 keV Fe X-rays within skin is limited, and our previous work has shown that Fe of depth greater than 0.5 mm does not contribute significantly to the signal measured by the pXRF instrument [33]. If elevated Fe levels are located within the epidermis, then the majority of Fe content in the skin of both rats and humans should be measurable by the ^{109}Cd pXRF system. Consequently, the rationale behind this study is that the disparity in skin thickness between human and rat skin is unlikely to significantly impact XRF measurements, making rat skin a viable model for studying the potential performance of the ^{109}Cd pXRF system for measurements of Fe overload in human skin.

2. Materials and methods

2.1. Sample preparation

The skin samples used in this study were obtained from rats that were loaded with Fe in a prior study [32]. As previously discussed, that study aimed to determine whether Fe loading via intraperitoneal injection resulted in elevated levels of Fe in skin. To briefly summarise the information from that published study: groups of male Wistar rats, a total of 32 animals, purchased from Charles River Laboratories, were injected intraperitoneally with Fe dextran (ANEM-X 100- iron injection, Aspen Veterinary Resources, Ltd.) over a period of three weeks followed by an eight day pause to allow Fe levels to reach equilibrium. A control group of rats were injected intraperitoneally with deionized water. The rats were fed a standard rodent diet and permitted to freely drink deionized water. No health information e.g. animal weight was provided in the publication about the rats as a consequence of iron dosing.

The dosing regime showing groups of rats and the total administered Fe doses are shown in Table 1. While the original study used 32 rats, viable skin samples were not available for all rats from the archive, and so 28 samples from 28 rats i.e. one sample per rat, were measured in this work.

As discussed, after euthanasia skin samples were cut from the animals and archived in a −80 °C freezer. Samples were released to the authors of this work. Upon receipt of the stored samples, the skin hairs were removed, and the skin was cut into a 4 cm diameter circle to fit in a phantom holder (made of polylactic acid and printed with 3D printer) as described in the published ^{109}Cd pXRF system calibration procedure [3]. The rat skin was approximately 2 mm thick and included a little of the underlying fat layer. The skin was fitted into the phantom with a paraffin wax base underneath the skin to simulate the scattering properties expected from the tissue below the skin in a rat. Twenty-eight skin samples were prepared from twenty-eight different animals, ranging from 0 mg Fe^{2+}/kg dose (normal Fe levels) to 160 mg Fe^{2+}/kg dose (Fe overload).

3. Experimental measurements

3.1. Skin sample measurement with the ^{109}Cd pXRF system

The rat skin samples were measured with a ^{109}Cd pXRF system, which utilizes a silicon drift detector (SDD) and ^{109}Cd as the excitation source. ^{109}Cd decays by electron conversion to ^{109}Ag and emits a series of characteristic silver X-rays ranging in energy from 22.0 keV ($K\alpha_2$) to 25.5 keV ($K_{\beta 2}$).

Characteristic Fe X-rays are produced when skin samples are irradiated with the approximately 22 and 25 keV silver X-rays from the source, and the detector (which is arranged in a backscatter geometry) measures the emitted Fe Kα X-rays as shown in Fig. 2.

Full details of the system were previously published [33,3]. Briefly, the source was collimated in a source holder and consequently irradiated a 1 cm diameter circle of the sample [33]. Each sample was measured for a real time measurement of 1800 s. The signals were amplified and analyzed by an Ortec Digital Gamma Ray Spectrometer (DSPEC, Ortec, Oregon United States) with Gamma Vision software. Calibration was performed against Fe-doped aqueous phantoms. The Fe X-ray peak areas were extracted from the XRF spectrum by fitting a mathematical model to the spectrum, with Gaussian functions and a linear background being used to model the X-ray peaks and background using the Marquardt method of analysis in Origin Pro software

Table 1
The total dose in mg Fe^{2+}/kg, the dosing regime and the number of measured skin samples.

Group	Total Administered Fe Dose as reported	Dosing regime (injections per week) as reported	Number of measured skin samples in this study
A	0 mg Fe^{2+}/kg	1 × 0.8 ml	8
B	80 mg Fe^{2+}//kg	1 × 0.8 ml	6
C	160 mg Fe^{2+}/kg	1 × 1.6 ml	5
D	160 mg Fe^{2+}/kg	2 × 0.8 ml	4
E	60 mg Fe^{2+}/kg	3 × 0.2 ml	2
F	75 mg Fe^{2+}/kg	3 × 0.25 ml	1
I	120 mg Fe^{2+}/kg	3 × 0.4 ml	2

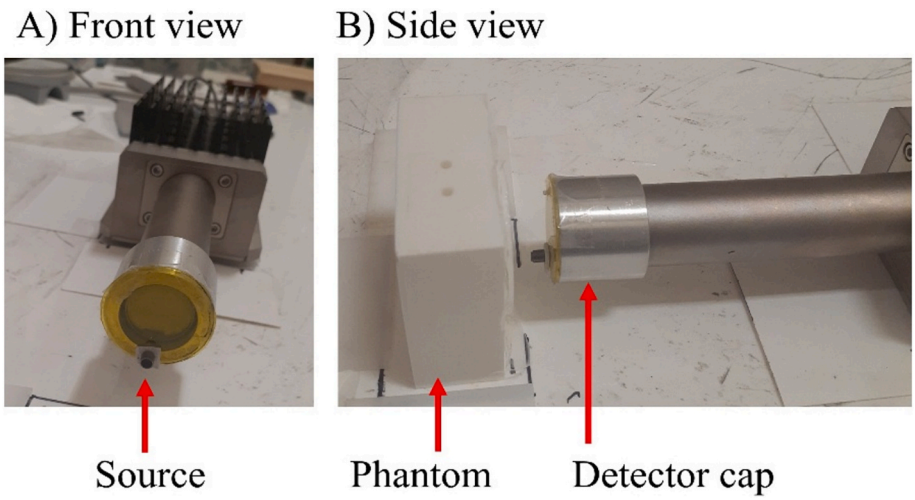

Fig. 2. Photographs of the experimental arrangement for measuring a rat skin sample using the ^{109}Cd pXRF system. View A shows the location of the source and collimator with respect to the detector face. View B shows the 'backscatter' geometry employed in a measurement.

(Northampton, Massachusetts, USA). The system delivers a skin dose of 1.1 mSv for an 1800 s measurement. Radioisotope measurements were performed under a permit issued by the Department of Health Physics at McMaster University. While the radioisotope is in a collimated holder, a radiation survey of emissions around the system was conducted to ensure that researcher doses were kept low and the ALARA principle (As Low As Reasonably Achievable) was followed for all measurements.

3.2. Measurement with the laboratory XRF system

The skin samples were also measured with a laboratory-based XRF system that was originally designed for studies of elemental distributions in cancer tissues [46,47] and which was utilized in the initial rat Fe loading study [32]. The laboratory XRF system utilizes a silicon drift detector (almost identical to that used in the ^{109}Cd-based system), but in the laboratory system, the fluorescing source is a molybdenum target microfocus X-ray tube that produces an approximately monochromated beam of energy approximately 17.5 keV. The beam is focused using a multilayer x-ray optical device (AXO Dresden, GmbH, Germany; resolution for Mo-Kα 1 %) to a size of 2 mm × 2 mm incident on the sample. The samples were placed in a sample holder and covered with 4 μm thick Ultraline X-ray film on both sides. The detector was mounted at an angle of 90° to the incident beam, and samples were mounted at 45° to the beam and to the detector. Each sample was measured for a live time of 1 h. The laboratory system is encased by a shielding box that is attached to the room infrastructure. It can only measure small samples and is not suitable for in vivo measurements.

3.3. Normalization to nickel

There was a prominent nickel (Ni) peak in the spectra obtained from both the ^{109}Cd pXRF and laboratory XRF systems due to the presence of nickel in the SDD detectors. The area of the Fe Kα peak and the area of the Ni Kα peak are both extracted from the spectrum in each system. The Fe Kα peak was normalized to the Ni Kα peak, as we have shown in previous work using the ^{109}Cd system [4] that this reduces the effect of phantom distance on the results in the ^{109}Cd XRF system. In addition to the Ni peak, as the laboratory XRF system is in an enclosed shielding box, a prominent argon peak arising from air is observed. The earlier study [32] utilized the argon peak for normalization purposes and measured each sample once. Consequently, to enhance comparability, each sample was only measured once using the ^{109}Cd pXRF system.

4. Results

4.1. Features in rat skin and phantom spectra

The ^{109}Cd pXRF system spectrum obtained from a rat skin sample (of estimated concentration 10 μg Fe/g) and a 10 μg Fe/g calibration phantom, both measured for 1800 s, are compared in Fig. 3. The concentration of the rat skin was estimated by dividing the Fe/Ni x-ray peak ratio obtained from the rat skin spectrum by the slope of the calibration line of Fe/Ni ratio versus Fe concentration obtained using Fe-doped phantoms. The spectra are similar, but the background under the Fe and Ni Kα X-rays in the 10 μg Fe/g phantom spectrum is higher than the background under the Fe and Ni Kα X-rays in the rat skin sample. The ratio of the backgrounds is a factor of 1.4. However, while the background appears larger in the phantom spectrum, the uncertainties in the measurements of the rat skin sample (not dosed with Fe) and a 10 μg/g water-based phantom are not significantly different.

The average measurement uncertainty of the rat skin samples was 11.0 ± 2.8 μg Fe/g while the average measurement uncertainty of the phantoms was 10.0 ± 1.8 μg Fe/g, respectively. In general, while the background may be larger, the spectral shape and measurement

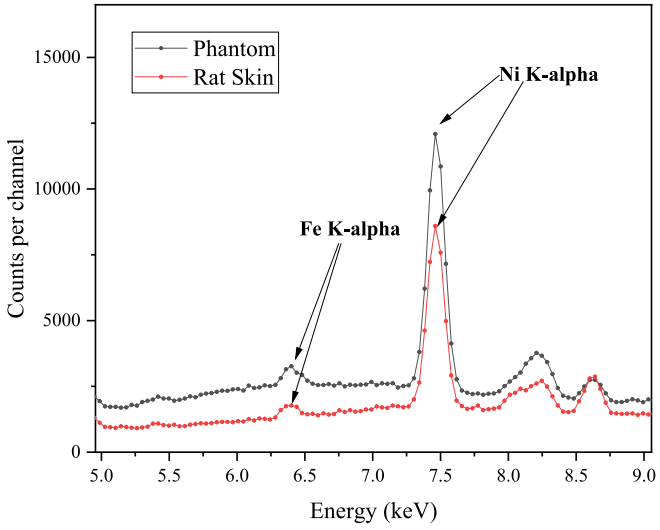

Fig. 3. Comparison of a 10 μg/g Fe phantom spectrum with an individual rat skin measurement spectrum.

uncertainty suggest that the water-based phantoms are good representation of rat skin Fe measurement spectra. However, the accuracy of the ^{109}Cd pXRF system has been previously published [33] and it has been shown, through Monte Carlo modelling, that a limitation of the phantoms may be that they are water-based phantoms with homogeneously distributed Fe content. This may not be an accurate model of the Fe distribution in the rat skin, which likely has higher Fe content at the skin surface. However, in the earlier study using pigskin [33], it was concluded that the system could be considered to be accurate over a range of Fe concentrations, although a correction factor may be necessary in some applications.

4.2. Ability of the ^{109}Cd pXRF system to predict rat dosage level

The rats whose skin was measured in this study received different doses of injected Fe as previously summarised in Table 1. In order to determine whether the ^{109}Cd pXRF system can distinguish between the Fe levels of the different dose groups, t-tests were applied between groups which followed the same dosing regime of one 0.8 ml injection per week but with different levels of iron. These three groups all had five or more animals. Testing was therefore performed for groups A, B and C, who had received doses of 0, 80 and 160 mg Fe^{2+}/kg, respectively. Each rat group distribution was tested for normality using Anderson-Darling methods with a rejection level of $p = 0.05$. The mean of group B (83.4 ± 13.8 μg Fe/g) was found to be significantly higher than the mean of group A (10.7 ± 1.3 μg Fe/g, $p < 0.003$) and the mean of group C (197.8 ± 7.2 μg Fe/g) was found to be significantly higher than the mean of group B, ($p < 0.0002$). The ^{109}Cd pXRF system was, therefore, able to distinguish between three different groups (each with 5 or more than 5 animals) who had been dosed following the same regime with Fe dosage steps of 80 mg Fe^{2+}/kg from 0 to 160 mg Fe^{2+}/kg.

To further test the ability of the ^{109}Cd pXRF system to distinguish between Fe dosage levels, and to include data from dosage groups with different dosing patterns with less than 5 animals, a linear regression was performed of group mean ^{109}Cd pXRF measurement of Fe content versus group Fe dosage level as shown in Fig. 4. This meant that measurements of animals from two different groups who were treated to the same total level of 160 mg Fe^{2+}/kg using different dosing regimes were tested together. A two-tailed *t*-test of the mean Fe levels in the two groups of animals found that the iron levels were not significantly different between dosing regime groups ($p = 0.07$). The measured skin Fe level was found to be strongly correlated with group dosage level (R^2 of 0.88) and increases by 1 μg Fe/g per mg/kg of injected Fe^{2+} dose. The regression is significant at the 95 % confidence level ($p = 0.05$).

The intercept 5.1 ± 15.6 μg Fe/g. was not found to be significantly different from zero. Using the variance data from t-tests, we can assume a standard deviation of approximately 30 μg Fe/g in the mean estimate of Fe content in a group of Fe-dosed rats. This suggests that a group of five animals with mean skin levels of approximately 40 μg Fe/g) would be identified as being Fe-dosed. This corresponds to a dose of 35 mg Fe^{2+}/kg. A ^{109}Cd pXRF Fe skin measurement can thus identify rat groups treated with Fe and distinguish them from a group of control animals even at the lowest doses measured in this study.

The system can thus distinguish between groups of rats, and to test the ability of the system to determine whether an individual rat has been dosed with Fe, a regression was performed of individual rat skin Fe levels measured by the ^{109}Cd pXRF system in μg Fe/g against the Fe dose delivered to rats in mg Fe^{2+}/kg. The plot of the regression is shown in Fig. 5. The two variables were strongly correlated, $r^2 = 0.83$, and the relationship was highly significant, $p < 0.0001$. Like the correlations between group skin Fe and dosage levels, the slope predicts that individual rat skin Fe levels will increase by 1 μg Fe/g per mg/kg of Fe^{2+} dose. The intercept was 7.7 ± 9.2 μg Fe/g. This suggests that the ^{109}Cd pXRF system can determine whether an individual rat has been dosed with Fe, using this regression curve, if the skin level is above approximately 25 μg Fe/g. This equates to an Fe dose of 18 mg Fe^{2+}/kg. The individual rat prediction is better than the group prediction because the regression data for individual animals is more precise than the regression data for the groups. The system can thus identify whether an individual animal has Fe levels that are above 'normal' for all dose levels in this study.

4.3. ^{109}Cd pXRF system comparison to laboratory XRF system

The rat samples' skin Fe concentrations were measured with both the laboratory XRF system and the ^{109}Cd pXRF system because the laboratory system had been used in prior published rat dosing studies [13]. It had been found in those studies that measurements of Fe levels in skin samples using the laboratory system could be correlated to Fe levels in liver samples from the same animal. We compared the ^{109}Cd pXRF skin estimates to the laboratory skin estimates, to assess more directly whether the ^{109}Cd pXRF measurements could be used as a surrogate for liver Fe measurement, our argument being: pXRF skin Fe measurement ∝ laboratory XRF skin Fe measurement ∝ laboratory XRF liver Fe measurement. The Fe/Ni ratio obtained for rat skin samples by the ^{109}Cd

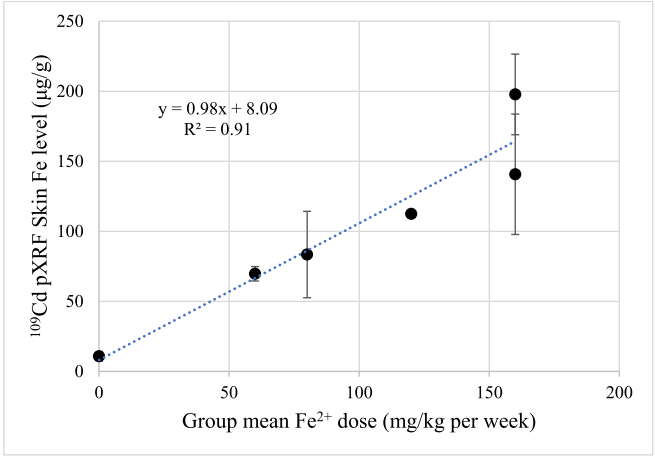

Fig. 4. The plot of the regression of group average Fe concentration in units of μg Fe/g wet weight measured in rat skin by ^{109}Cd pXRF versus total administered Fe^{2+} dose to rats in mg/kg. Plotted uncertainty data are the standard deviation of the mean. Rats dosed to 160 Fe^{2+} mg/kg were dosed using two different dosing regimes hence there are two 160 Fe^{2+} mg/kg dose groups. The different dose regime groups are shown in Table 1.

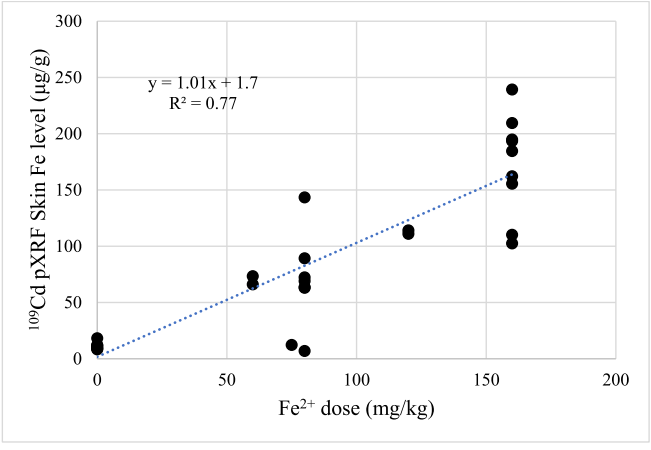

Fig. 5. A plot of the regression of individual rat skin Fe concentration measured in units of μg per g wet weight by ^{109}Cd pXRF versus individual rat total Fe dose administered in mg Fe^{2+}/kg. Rats dosed to a total dose of 160 mg Fe^{2+}/kg were dosed using two different dosing regimes. The different dose regime groups are shown in Table 1.

pXRF system was therefore regressed against the laboratory system Fe/Ni ratio from the same samples, as shown in Fig. 6. The graph shows a strong linear correlation between the system measurements with a coefficient of determination (R^2) of 0.85. The relationship is highly statistically significant ($p < 0.0001$).

This initial regression analysis assumes that the laboratory XRF estimates have no or negligible measurement uncertainty, which is not valid. The uncertainties in the laboratory estimates are smaller than for the ^{109}Cd pXRF system estimates, but they are not negligible. To assess the limits of the relationship, the laboratory XRF results were then regressed against the ^{109}Cd pXRF results, and the equation rearranged to provide a relationship for the ^{109}Cd pXRF in terms of the laboratory XRF. The results are shown in Table 2 and the regression lines can be seen in Fig. 6. While the regression of pXRF versus laboratory has an intercept that is significantly different than zero, it is not significant when regressed in the other direction, so there is little evidence of an offset in the relationship between the two systems. The results indicate a linear relationship between the ^{109}Cd pXRF and the laboratory skin Fe estimates and as the laboratory skin Fe estimates are linearly correlated with the liver estimates, then the ^{109}Cd pXRF skin measurements are expected be correlated with the liver Fe levels in these animals. A measurement of elevated skin Fe level by the ^{109}Cd pXRF system can potentially be assumed to be a surrogate measurement indicating elevated liver Fe levels in Fe dosed animals.

5. Discussion

Efficient, effective and minimally invasive monitoring of Fe levels in real time is essential for management of patients with Fe overload. The results of the ex vivo work indicate that the ^{109}Cd pXRF system shows potential not only for use in rats with varying degrees of iron overload over time but is likely able to monitor changes in individual animals. However, the level at which the system can determine 'elevated' Fe in an individual rat in vivo will depend on the establishment of a strong set of baseline in vivo low Fe level data against which an individual rat's Fe level can be compared. The ability to determine the dose an animal received by a measurement of skin Fe alone, will depend on the establishment of a precise calibration line obtained from measurements in an in vivo study. This work shows that such a study may be worth undertaking.

However, the ultimate goal is to create a device for in vivo measurements in humans, as opposed to a pre-clinical system for studies in rats. Whether this work indicates potential in human measurements strongly depends on how well measurements of rat skin indicate the ability to measure levels in human skin. The question of whether these measurements in rat skin are an indication of the performance of this system in human measurements depends on how well rat skin matches human skin and whether the ^{109}Cd pXRF system measures the same layers of skin in the two species.

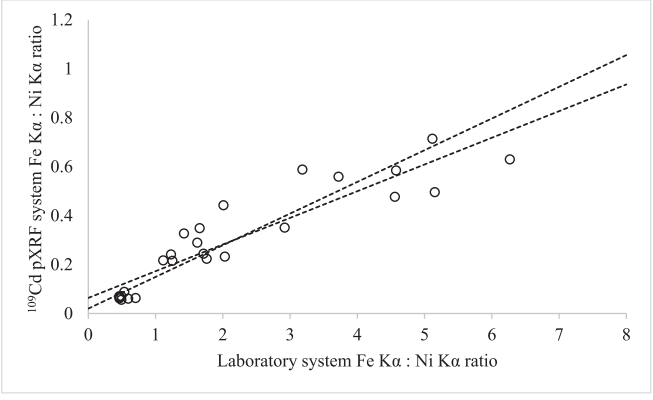

Fig. 6. A plot of the results of the regression of the ^{109}Cd pXRF system Fe Kα x-ray: Ni Kα ratio versus the laboratory XRF Fe Kα x-ray: Ni Kα ratio and vice versa for rat skin Fe measurements. The regression was performed in both directions to account for the fact that both variables have uncertainties.

Table 2
The slopes and intercepts determined from the regression of ^{109}Cd pXRF measurements versus laboratory XRF measurements obtained from regressions of y against x and x against y.

Regression	Slope	Intercept
pXRF versus laboratory	0.110 ± 0.010	0.060 ± 0.025
Laboratory versus pXRF	0.129 ± 0.011	0.019 ± 0.011

Rat skin is notably thinner and more loosely attached compared to human skin. However, the skin types do share fundamental similarities in structure and function. Rats and humans both have skin composed of layers: at the surface the stratum corneum, then the rest of the epidermis, dermis and hypodermis. We argue that the similarities between human skin and rat skin are such that the system would measure normal human skin as well as it can measure rat skin. However, it is known that the ^{109}Cd pXRF system predominantly measures Fe at the surface layer of the skin [33]. Differences between rat and human dermis are possibly less important than differences between rat and human epidermis. Rat and human epidermis show some overlap in skin thickness and structure.

The question remains as to whether the distribution of Fe in skin will be the same in rats and humans under conditions of both health and pathologic Fe accumulation. Overall, studies of Fe distributions in skin are limited. There is some data on the distribution of Fe in pig [33] or human skin [36,48–52]. Several of these publications suggest that levels in the stratum corneum may depend on the health status of the person. Generally, they indicate that Fe is concentrated at the epidermal/dermal boundary in healthy individuals but may be increased in the epidermis and stratum corneum under conditions of disease such as psoriasis or eczema. Levels also increase in the upper layers of the skin in patients with hemochromatosis, but the Fe distribution appears to depend on the treatment status of the patient. Our own work utilizing synchrotron μXRF measurements to analyze Fe distribution in pig skin [33] has shown increased levels of Fe in the superficial layers of the skin, with the thickness of the Fe layer being up to 100 μm thick (Fig. 7).

Our prior simulations of Fe distributions in pig skin samples have suggested that when a high Fe layer is present at the skin's surface, the overall XRF signal predominantly measures the Fe concentration in the front layer, with lesser contribution from the lower Fe concentrations in the deeper layers [33].

If high Fe concentrations resulting from overload are localized at the skin's surface, it is plausible to infer that the overall thickness difference between human and rat skin would have a negligible impact on ^{109}Cd pXRF results, and these rat skin measurements likely indicate that the ^{109}Cd pXRF system can distinguish between high and low Fe levels in humans. However, further work in either a small human in vivo feasibility study or ex vivo skin studies will be required to validate this hypothesis.

6. Conclusion

A ^{109}Cd pXRF system for measurement of Fe in skin was found to be able to differentiate between normal and Fe-overloaded rat skin samples. The system was both able to differentiate between the skin Fe levels of small groups of rats loaded with different levels of Fe and, further, identify whether an individual rat was from an Fe-loaded or normal group based on measurement of skin Fe level. Rat skin Fe measurements using the ^{109}Cd pXRF system were found to be highly correlated with a laboratory XRF system which had determined that rat skin levels were correlated with liver Fe levels in Fe overloaded rats. The results indicate that the ^{109}Cd pXRF system measurements of skin Fe should be a surrogate measurement for elevated liver Fe levels in rats. Further work is

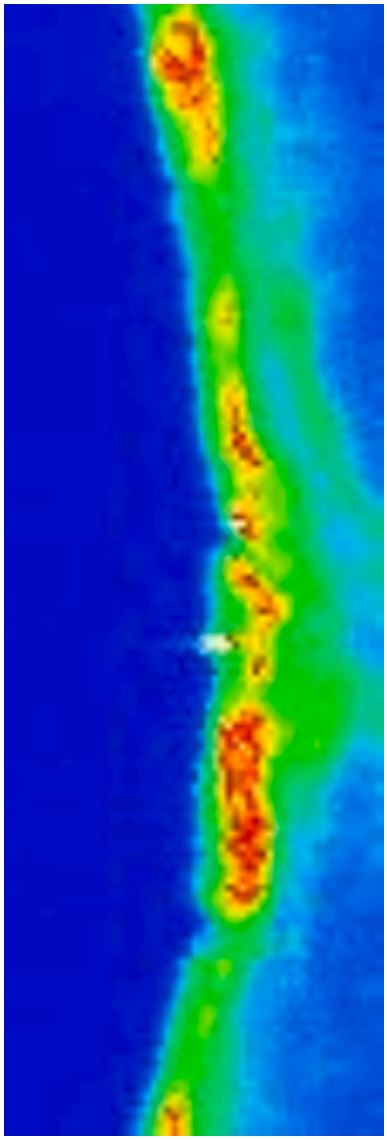

Fig. 7. A 5 μm resolution μXRF map of Fe in the surface of pigskin diffused with saline collected in the BioXAS beamline at the Canadian Light Source. Red indicates higher Fe levels and blue lower Fe levels. The skin surface is in the centre of the image and the scan moves deeper into the skin towards the right. The higher Fe layer at the skin surface is 80–100 μm thick. (For interpretation of the references to colour in this figure legend, the reader is referred to the web version of this article.)

required to verify the performance of the system in human populations.

CRediT authorship contribution statement

Sami Ullah Bangash: . **Fiona E. McNeill:** Writing – review & editing, Validation, Supervision, Resources, Project administration, Methodology, Funding acquisition, Formal analysis, Conceptualization. **Michael J. Farquharson:** Writing – review & editing, Supervision, Resources, Project administration, Methodology, Funding acquisition, Formal analysis, Conceptualization. **Bruce Wainman:** Writing – review & editing, Validation, Conceptualization. **Michelle Zeller:** Writing – review & editing, Validation, Conceptualization.

Declaration of competing interest

The authors declare that they have no known competing financial interests or personal relationships that could have appeared to influence the work reported in this paper.

Acknowledgements

The Government of Canada's NSERC Discovery program provided funding for this research.

Data availability

Data will be made available on request.

References

[1] H.-W. Yuen and W. G. Gossman, Iron Toxicity, StatPearls, Jun. 2022, Accessed: Apr. 27, 2023 [Online], Available: https://www.ncbi.nlm.nih.gov/books/NBK459224/.
[2] M.J. Farquharson, A.P. Bagshaw, Monitoring body iron burden using X-ray fluorescence (XRF), Radiat. Phys. Chem. 61 (3–6) (2001) 599–601, https://doi.org/10.1016/S0969-806X(01)00344-9.
[3] S.U.K. Bangash, F.E. McNeill, M.J. Farquharson, D.R. Chettle, Feasibility of a 109Cd-based portable XRF device for measuring skin iron concentration in anaemic and β−Thalassaemic patients, Biomed. Phys. Eng. Express 8 (6) (2022) 065034, https://doi.org/10.1088/2057-1976/AC9E02.
[4] D.R. Chettle, F.E. McNeill, Elemental analysis in living human subjects using biomedical devices, Physiol. Meas. 40 (12) (2019) 12TR01, https://doi.org/10.1088/1361-6579/AB6019.
[5] I. Szalóki, D.G. Lewis, C.A. Bennett, A. Kilic, Application of the fundamental parameter method to the in vivo x-ray fluorescence analysis of Pt, Phys. Med. Biol. 44 (5) (1999) 1245, https://doi.org/10.1088/0031-9155/44/5/012.
[6] R.G. Figueroa, I.R. Chávez, E. Bonzi, In vivo EDXRF scanning analysis of human nail, X-Ray Spectrom. 43 (6) (2014) 338–344, https://doi.org/10.1002/XRS.2560.
[7] M.R. Gherase, D.E.B. Fleming, Fundamental parameter approach to XRF spectroscopy measurements of arsenic in polyester resin skin phantoms, X-Ray Spectrom. 37 (5) (2008) 482–489, https://doi.org/10.1002/XRS.1051.
[8] P.J. Parsons, Y.Y. Zong, M.R. Matthews, Development of bone-lead reference materials for validating in vivo Xrf measurements, Adv. X-Ray Anal. 38 (1994) 625–632, https://doi.org/10.1154/S0376030800018322.
[9] E. Da Silva, B. Kirkham, D.V. Heyd, A. Pejović-Milić, Pure hydroxyapatite phantoms for the calibration of in vivo x-ray fluorescence systems of bone lead and strontium quantification, Anal. Chem. 85 (19) (2013) 9189–9195, https://doi.org/10.1021/AC401877D/ASSET/IMAGES/MEDIUM/AC-2013-01877D_0006.GIF.
[10] L. Ahlgren, S. Mattsson, An X-ray fluorescence technique for in vivo determination of lead concentration in a bone matrix, Phys. Med. Biol. 24 (1) (1979) 136, https://doi.org/10.1088/0031-9155/24/1/011.
[11] M. Hansson, In vivo X-ray fluorescence analysis (XRF), Phys. Med. Biol. 49 (7) (2007) 387–2019.
[12] L. Ahlgren, B. Haeger-Aronsen, S. Mattsson, A. Schuetz, In-vivo determination of lead in the skeleton after occupational exposure to lead, Occup. Environ. Med. 37 (2) (1980) 109–113, https://doi.org/10.1136/OEM.37.2.109.
[13] L.J. Somervaille, et al., In vivo tibia lead measurements as an index of cumulative exposure in occupationally exposed subjects, Occup. Environ. Med. 45 (3) (1988) 174–181, https://doi.org/10.1136/OEM.45.3.174.
[14] L.J. Somervaille, et al., In vivo measurements of bone lead-a comparison of two X-ray fluorescence techniques used at three different bone sites, Phys. Med. Biol. 34 (12) (1989) 1833, https://doi.org/10.1088/0031-9155/34/12/007.
[15] J.M. O'Meara, D.R. Chettle, F.E. McNeill, C.E. Webber, In vivo X-ray fluorescence (XRF) measurement of uranium in bone, Appl. Radiat. Isot. 49 (5–6) (1998) 713–715, https://doi.org/10.1016/S0969-8043(97)00091-2.
[16] J.M. O'Meara, D.R. Chettle, F.E. McNeill, C.E. Webber, The feasibility of measuring bone uranium concentrations in vivo using source excited K x-ray fluorescence, Phys. Med. Biol. 42 (6) (1997) 1109, https://doi.org/10.1088/0031-9155/42/6/008.
[17] A.J. Specht, M.G. Weisskopf, L.H. Nie, Theoretical modeling of a portable x-ray tube based KXRF system to measure lead in bone, Physiol. Meas. 38 (3) (2017) 575, https://doi.org/10.1088/1361-6579/AA5EFE.
[18] L.H. Nie, S. Sanchez, K. Newton, L. Grodzins, R.O. Cleveland, M.G. Weisskopf, In vivo quantification of lead in bone with a portable x-ray fluorescence system—methodology and feasibility, Phys. Med. Biol. 56 (3) (2011) N39, https://doi.org/10.1088/0031-9155/56/3/N01.
[19] X. Zhang, A.J. Specht, E. Wells, M.G. Weisskopf, J. Weuve, L.H. Nie, Evaluation of a portable XRF device for in vivo quantification of lead in bone among a US population, Sci. Total Environ. 753 (2021) 142351, https://doi.org/10.1016/J.SCITOTENV.2020.142351.
[20] A.J. Specht, A.S. Dickerson, M.G. Weisskopf, Comparison of bone lead measured via portable x-ray fluorescence across and within bones, Environ. Res. 172 (2019) 273–278, https://doi.org/10.1016/J.ENVRES.2019.02.031.
[21] X. Zhang, A.J. Specht, E.M. Wells, M.G. Weisskopf, J. Weuve, L.H. Nie, In vivo quantification of bone lead and strontium using portable X-ray fluorescence (XRF), ISEE Conf. Abstr. 2021 (1) (2021), https://doi.org/10.1289/ISEE.2021.P-325.
[22] X. Zhang, E.M. Wells, A.J. Specht, M.G. Weisskopf, J. Weuve, L.H. Nie, In vivo quantification of strontium in bone among adults using portable x-ray

fluorescence, J. Trace Elem. Med Biol. 74 (2022) 127077, https://doi.org/10.1016/j.jtemb.2022.127077.
[23] A.J. Specht, et al., XRF-measured bone lead (Pb) as a biomarker for Pb exposure and toxicity among children diagnosed with Pb poisoning, Biomarkers 21 (4) (2016) 347–352, https://doi.org/10.3109/1354750X.2016.1139183.
[24] A.J. Specht, M. Weisskopf, L.H. Nie, Portable XRF technology to quantify Pb in bone in vivo, J. Biomarkers 2014 (1) (2014) 398032, https://doi.org/10.1155/2014/398032.
[25] A.J. Specht, F. Mostafaei, Y. Lin, J. Xu, L.H. Nie, Measurements of strontium levels in human bone in vivo using portable X-ray fluorescence (XRF), 71(8) (2017) 1962–1968, doi: 10.1177/0003702817694383.
[26] B. Laura, Studies to improve the in vivo measurement of strontium by X-ray fluorescence, 2024, Accessed: Mar. 02, 2025 [Online], Available: https://macsphere.mcmaster.ca/handle/11375/30090.
[27] M. Estevam, C.R. Appoloni, Use of portable X-ray fluorescence (PXRF) in vivo as an alternative technique for the assessment of iron levels in patients with thalassemia and hemochromatosis, Health Phys. 104 (2) (2013) 132–138, https://doi.org/10.1097/HP.0B013E3182667721.
[28] M.J. Farquharson, D.A. Bradley, The feasibility of a sensitive low-dose method for the in vivo evaluation of Fe in skin using K-shell x-ray fluorescence (XRF), Phys. Med. Biol. 44 (4) (1999) 955, https://doi.org/10.1088/0031-9155/44/4/011.
[29] M. Estevam, C.R. Appoloni, The in vivo use of portable X-ray fluorescence as an alternative technique for the accompaniment of iron levels in patients with iron loading, Rev. Bras. Hematol. Hemoter. 31 (3) (2009) 153–159, https://doi.org/10.1590/S1516-84842009005000043.
[30] D.A. Bradley, M.J. Farquharson, X-ray fluorescence and the in vivo evaluation of Fe, Cu and Zn in skin, J. Radioanal. Nucl. Chem. 244 (1) (2000) 213–217, https://doi.org/10.1023/A:1006757424682/METRICS.
[31] M. Estevam, C.R. Appoloni, In vivo evaluation of Fe in human skin employing X-ray fluorescence methodology (XRF), AIP Conf. Proc. 884 (1) (2007) 468, https://doi.org/10.1063/1.2710631.
[32] E. Dao, M.P. Zeller, B.C. Wainman, M.J. Farquharson, Feasibility of the use of a handheld XRF analyzer to measure skin iron to monitor iron levels in critical organs, J. Trace Elem. Med Biol. 50 (2018) 305–311, https://doi.org/10.1016/j.jtemb.2018.07.024.
[33] S.U. Bangash, F.E. McNeill, M.J. Farquharson, Investigation of the accuracy of a portable 109Cd XRF system for the measurement of iron in skin, Biomed. Phys. Eng. Express 10 (3) (2024) 035032, https://doi.org/10.1088/2057-1976/AD3D60.
[34] M. Estevam, et al., Trypanosoma cruzi: in vivo evaluation of iron in skin employing X-ray fluorescence (XRF) in mouse strains that differ in their susceptibility to infection, FEMS Immunol. Med. Microbiol. 64 (3) (2012) 334–342, https://doi.org/10.1111/J.1574-695X.2011.00917.X.
[35] M.J. Farquharson, A.P. Bagshaw, J.B. Porter, R.D. Abeysinghe, The use of skin Fe levels as a surrogate marker for organ Felevels, to monitor treatment in cases of iron overload, Phys. Med. Biol. 45 (5) (2000) 1387, https://doi.org/10.1088/0031-9155/45/5/320.
[36] T. Pinheiro, et al., Distribution and quantitation of skin iron in primary haemochromatosis: correlation with total body iron stores in patients undergoing phlebotomy, Acta Derm. Venereol. 94 (1) (2014) 14–19, https://doi.org/10.2340/00015555-1601.
[37] R. Gorodetsky, A. Goldfarb, I. Dagan, E.A. Rachmilewitz, Noninvasive analysis of skin iron and zinc levels in β-thalassemia major and intermedia, J. Lab. Clin. Med. 105 (1) (1985) 44–51, https://doi.org/10.5555/URI:PII:0022214385900873.
[38] I. Youssry et al., Skin iron concentration: a simple, highly sensitive method for iron stores evaluation in thalassemia patients, 31(3) (2009) 357–365, doi: 10.1080/03630260701503833.
[39] M.Y. Wells et al., Histomorphology and vascular lesions in dorsal rat skin used as injection sites for a subcutaneous toxicity study, doi: 10.1177/0192623309357953.
[40] R.L. Maynard, N. Downes, The skin or the integument, Anat. Histol. Embryol. (2019) 303–315, https://doi.org/10.1016/B978-0-12-811837-5.00024-1.
[41] P.M. Treuting, S.M. Dintzis, K.S. Montine, Comparative anatomy and histology : a mouse, rat and human atlas, p. 552.
[42] Skin-Layer, Structure, and Functions, https://www.geeksforgeeks.org/skin/(accessed Jan. 08, 2024).
[43] H. Pinkus, Anatomy of the skin, Dermatologica 108 (1) (1954) 37–59, https://doi.org/10.1159/000256718.
[44] S. Zaki Soliman Fakeeh Hospital, J. Cytol Histol, S. Mohamed Zaki, Characteristics of the skin of the female albino rats in different ages: histological, morphometric and electron microscopic study, Artic. J. Cytol. Histol. S (2015) 3, https://doi.org/10.4172/2157-7099.S3-004.
[45] D.A. Lintzeri, N. Karimian, U. Blume-Peytavi, J. Kottner, Epidermal thickness in healthy humans: a systematic review and meta-analysis, J. Eur. Acad. Dermatol. Venereol. 36 (8) (2022) 1191–1200, https://doi.org/10.1111/JDV.18123.
[46] S. Darvish-Molla, A. Al-Ebraheem, M.J. Farquharson, The identification and differentiation of secondary colorectal cancer in human liver tissue using X-ray fluorescence, coherent scatter spectroscopy, and multivariate analysis, Appl. Spectrosc. 68 (1) (2014) 79–87, https://doi.org/10.1366/13-07047.
[47] M.J. Farquharson, A. Al-Ebraheem, S. Cornacchi, G. Gohla, P. Lovrics, The use of X-ray interaction data to differentiate malignant from normal breast tissue at surgical margins and biopsy analysis, X-Ray Spectrom. 42 (5) (2013) 349–358, https://doi.org/10.1002/XRS.2455.
[48] Y. Werner-Linde, J. Pallon, B. Forslind, Physiologically important trace elements of paralesional psoriatic skin, Scanning Microsc. 12 (4) (1998) 599–608.
[49] J. Pallon, K.G. Malmqvist, Y. Werner-Linde, B. Forslind, Pixe analysis of pathological skin with special reference to psoriasis and atopic dry skin, Cell. Mol. Biol. (Noisy-le-Grand) 42 (1) (1996) 111–118.
[50] P. Moretto, J.E. Surleve-Bazeille, D. Lieu, C. Michelet, P. Stoedzel, Microanalysis of the human skin structure: preliminary results, Nucl. Instrum. Meth. B 158 (1–4) (1999) 386–392, https://doi.org/10.1016/S0168-583X(99)00346-8.
[51] Y. Inoue, et al., ZIP2 protein, a zinc transporter, is associated with keratinocyte differentiation, J. Biol. Chem. 289 (31) (2014) 21451–21462, https://doi.org/10.1074/jbc.M114.560821.
[52] I. Guinote, et al., Using skin to assess iron accumulation in human metabolic disorders, Nucl. Instruments Methods Phys. Res. Sect. B Beam Interact. Mater. Atoms. 249 (1–2) (2006) 697–701, https://doi.org/10.1016/J.NIMB.2006.03.120.